

# Model predictive control of high voltage direct current based on voltage source converter transmission system

Nouir Ahmed<sup>1</sup>, Zebirate Soraya<sup>1,2</sup>, Chaker Abdelkader<sup>1,3</sup>

<sup>1</sup>Department of Electrical Engineering, National School of Polytechnics Oran (ENPO) Maurice Audin, Oran, Algeria

<sup>2</sup>Institute of Industrial Maintenance and Security, Oran, Algeria

<sup>3</sup>Simulation, Commande, Analyse et Maintenance des Réseaux Electriques (SCAMRE) Laboratory, Oran, Algeria

## Article Info

### Article history:

Received Jun 13, 2022

Revised Nov 12, 2022

Accepted Nov 29, 2022

### Keywords:

Dynamic response

High voltage direct current

Model predictive control

Predictive control

Voltage source converter

## ABSTRACT

Model predictive control (MPC) has recently been ranked as one of the best modern technics of control for high voltage direct current (HVDC) based on voltage source converter (VSC) transmission systems, since it is a simple controller, understandable and can be implemented easily, also has a dynamic and fast response. The classic double closed loop PI controller has many disadvantages such as the difficulty in determining the  $K_p$ ,  $K_i$ , and  $K_d$  parameters as well as the couplings; It is also less robust against systems with slow dynamics and/or having a complex structure. This paper exposes a model predictive control for a two-level converter. Direct power control on rectifier-side based on model prediction and on the inverter-side AC current control strategy is proposed. The controller utilizes the identified model to anticipate the comportment of the output voltage of every switching state at each sampling frequency. At the next sampling interval, the optimum switching state is applied using the cost function as a reference point. The MPC method was verified by the tools of the MATLAB/Simulink software. The simulation results validate the feasibility and effectiveness of the presented control strategy.

This is an open access article under the [CC BY-SA](#) license.



## Corresponding Author:

Nouir Ahmed

Department of Electrical Engineering, National School of Polytechnics ORAN (ENPO) Maurice Audin

Route d'Es-Sénia, B.P. 1523 El M'Naouer, Oran, Algeria

Email: hmdlaid@gmail.com

## 1. INTRODUCTION

The direct current (DC) for long-distance power transmission began in 1954 once ASEA, build the first link with high-voltage direct-current (HVDC) lines. However, the DC's history appears before that. Thomas Edison failed to keep on against his rival the alternating current AC in the 1890s it became clear that ac was more efficient at transmitting electricity over long distances. On the other hand, due to the increase of electricity consumption through the world, the DC is nesting again between the branches granting a new spot [1]. Nowadays, power electronics are used to convert and control electrical energy. The growing consumption of electrical energy has prompted the development of new standards for evaluating energy quality and efficiency [2], [3]. Faced with the novelty of semiconductors, a whole new generation of control diagrams has been traced [4]. In the 1990s, the growth of semiconductors such as insulated-gate bipolar transistor and gate turn-off thyristor, had reached values allowing them to be used by voltage source converters (VSC). The very early VSC-based HVDC transmission line with a 50 MW underground cable was operational in 1999 on the island of Gotland; there are several names for these transmission cables such as HVDC plus, VSC-HVDC, and HVDC light [5]-[7]. The HVDC system requires the elaboration of rigorous control techniques of both active and reactive power flows, because it has several advantages such as a

decoupled and fast control of the power flow, the improvement of the power quality indicator and supply of isolated loads [8]-[13].

The model predictive control (MPC) shows a huge advancement in modern automatic control theory. At first, the process industry was the perfect field to study and apply the MPC, where it has been in use for many years ago [6]. Today, other fields put a lot of attention against the predictive control, such as electrical drives and power electronics [14]-[18]. The growing use of MPC is due to the better mathematical models for predicting the comportment of the controlled variables in electromechanical systems [14]. Moreover, the recent cutting edge technologies microprocessors can perform at high speed and low cost a large number of calculations required in MPC [19], [20]. The MPC method has been used in several power converters for its high dynamic performance, simple design and ability to regulate the AC signal directly without frequency conversion [21]-[26].

Recently, some recent research has found very interesting results of MPC predictive control. The article [18] draws up a table of some differences between the model predictive controller and the proportional-integral regulator and demonstrates the robustness of the predictive control through theoretical and experimental calculations. Zhang *et al.* [27] gives the mathematical modeling and the design of the MPC control strategy. Zhao *et al.* [28] details the MPC control of VSC-HVDC that powers passive networks.

In this article, we started with the discrete mathematical modeling of the two sides of the VC-HVDC system. Direct power control was applied on the rectifier part, while the alternative control based on a prediction model was used on the inverter part. In its simplest structure, the MPC control is more efficient due to the anticipation of the next values of the variables, which makes it more robust and more stable than the classical double closed-loop proportional integral (PI) control. The dynamic response speed is rapid, and the steady state and dynamic performance are both good. Finally, based on MATLAB/Simulink platform, we have built a VSC-HVDC system that powers a passive network, in order to confirm the suggested control strategy.

## 2. MATHEMATICAL MODEL OF THE VSC-based HVDC SYSTEM

Figure 1 gives the general structure of the VSC-based HVDC system. It consists mainly with three main parts: sending end, transmission line and receiving end. Where Table 1 shows in detail the components that consists in that system.

Table 1. System symbols designations

Item symbol	Meaning
$Z_{sj}$	Equivalent resistance of the AC system source
$L_j$	Commutation reactor inductance
$R_j$	Commutation reactor resistance
$u_j$	Three phase AC voltage
$i_j$	Three phase AC current
$u_{dc}$	DC voltage
$i_{dc}$	DC current that passes the DC link transmission line
$C$	DC capacitor

Where  $j=1, 2$  (1: rectifier station, 2: inverter station)

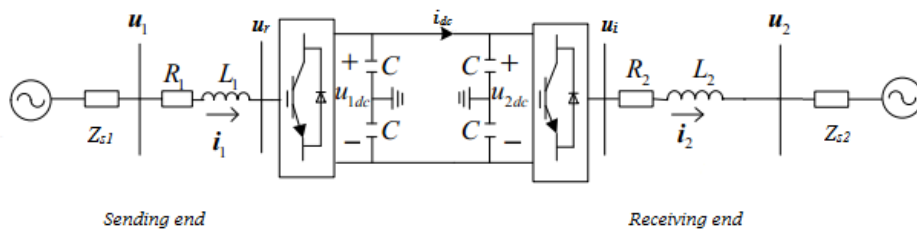


Figure 1. The general structure of VSC-HVDC system

### 2.1. Mathematical model of the rectifier side

According to Figure 1, (1) is determined by the KVL law, in a stationary three-phase coordinate system, a continuous mathematical model of the rectifier side can be obtained.

$$L_1 \frac{di_{1k}}{dt} = u_{1k} - R_1 i_{1k} - u_{rk} \quad (1)$$

Where  $k=a, b, c$ . To decouple currents and voltages, we change the frame by performing Clark transformation.

$$L_1 \frac{di_1}{dt} = u_1 - R_1 i_1 - u_r \quad (2)$$

Where  $i_1 = \begin{bmatrix} i_{1\alpha} \\ i_{1\beta} \end{bmatrix}$ ,  $u_1 = \begin{bmatrix} u_{1\alpha} \\ u_{1\beta} \end{bmatrix}$  and  $u_r = \begin{bmatrix} u_{r\alpha} \\ u_{r\beta} \end{bmatrix}$ . The current  $i_l$  can be expressed as a function of the current  $i_s$  as:

$$i_1 = \frac{2}{3} (i_{1a} + a i_{1b} + a^2 i_{1c}) = i_{1\alpha} + j i_{1\beta} \quad (3)$$

where  $a = e^{j(2\pi/3)}$ . Also, the voltages  $u_1$  and  $u_r$  are defined as (4).

$$u_1 = \frac{2}{3} (u_{1a} + a u_{1b} + a^2 u_{1c}) \quad (4)$$

The voltage  $u_r$  is given by  $u_{1dc}$  as:

$$u_r = S_{rec} * u_{1dc} \quad (5)$$

where  $S_{rec}$  is the switching state vector of the rectifier expressed by (6).

$$S_{rec} = \frac{2}{3} (S_{1a} + a S_{1b} + a^2 S_{1c}) \quad (6)$$

In this formula,  $S_{1k}$  is the switching function of the rectifier in the  $k$ -phase bridge arm, which is designed to work as mentioned in Table 2.

Discretization of (2):

$$i_1(k+1) = \left(1 - \frac{R_1 T_s}{L_1}\right) i_1(k) + \frac{T_s}{L_1} [u_1(k) - u_r(k)] \quad (7)$$

The discretization is obtained by approximating the derivative as the difference over one sampling period ( $T_s$ ):

$$\frac{di}{dt} \cong \frac{i(k+1) - i(k)}{T_s} \quad (8)$$

Table 2. Rectifier switching function

$S_{1k}$	Upper arm	Lower arm
0	OFF	ON
1	ON	OFF

## 2.2. Inverter side mathematical model

When the AC system is stable (Figure 1), the mathematical model of the inverter side can be obtained as:

$$L_2 \frac{di_{2k}}{dt} = -u_{2k} - R_2 i_{2k} + u_{ik} \quad (9)$$

where, the output voltage of the inverter is given by:

$$u_{ik} = u_{2dc} \left( S_{2k} - \frac{1}{3} \sum_{m=a,b,c} S_{2m} \right) \quad (10)$$

By performing the inverse Clark transformation, the  $\alpha\beta$  coordinate system of (9) can be obtained as:

$$L_2 \frac{di_2}{dt} = -u_2 - R_2 i_2 + u_{2dc} S_{inv} \quad (11)$$

where  $S_{inv} = \frac{2}{3} (S_{2a} + a S_{2b} + a^2 S_{2c})$ . Discretization of (11) using the first-order forward difference method yields:

$$i_2(k+1) = \left(1 - \frac{R_2 T_s}{L_2}\right) i_2(k) + \frac{T_s}{L_2} [u_i(k) - u_2(k)] \quad (12)$$

### 3. CONTROLLER DESIGN

#### 3.1. Rectifier side controller

Instantaneous predicted input powers are calculated by:

$$P_{in}(k+1) = \text{Re}\{u_1(k+1)\bar{i}_1(k+1)\} = u_{1\alpha}i_{1\alpha} + u_{1\beta}i_{1\beta} \quad (13)$$

$$Q_{in}(k+1) = \text{Im}\{u_1(k+1)\bar{i}_1(k+1)\} = u_{1\beta}i_{1\alpha} - u_{1\alpha}i_{1\beta} \quad (14)$$

where  $i_1(k+1)$  is the anticipated input current. About the grid fundamental frequency of the network, for a small sampling frequency, we can assume that  $u_1(k+1) \approx u_1(k)$ . A proportional integral regulator controls the intermediate circuit voltage. The control signal of the controller symbolizes the power required to balance the voltage error of the intermediate circuit.

$$P_{in}^* = (k_p + \frac{k_i}{s})(u_{1dc}^* - u_{1dc}) + P_{1dc} \quad (15)$$

Where  $P_{1dc} = u_{1dc}i_{dc} + P_{1c}$ , here  $P_{1c}$  is the active power demanded by the capacitor. At steady state we suppose that  $P_{1c} \approx 0$  thus  $P_{1dc} \approx u_{1dc}i_{dc}$ . So as to stabilize the powers at their setpoint values, the following objective function is expressed by:

$$g_{rec} = |Q_{in}^* - Q_{in}(k+1)| + |P_{in}^* - P_{in}(k+1)| \quad (16)$$

where  $P_{in}^*$  and  $Q_{in}^*$  are the active and reactive power setpoints respectively. The cost function  $g_{rec}$  summarizes the rectifier's desired performance: control the active power  $P_{in}$  and reduce the reactive power error. The block diagram and the designed Simulink model of the control strategy are given in Figures 2(a) and 2(b) respectively.

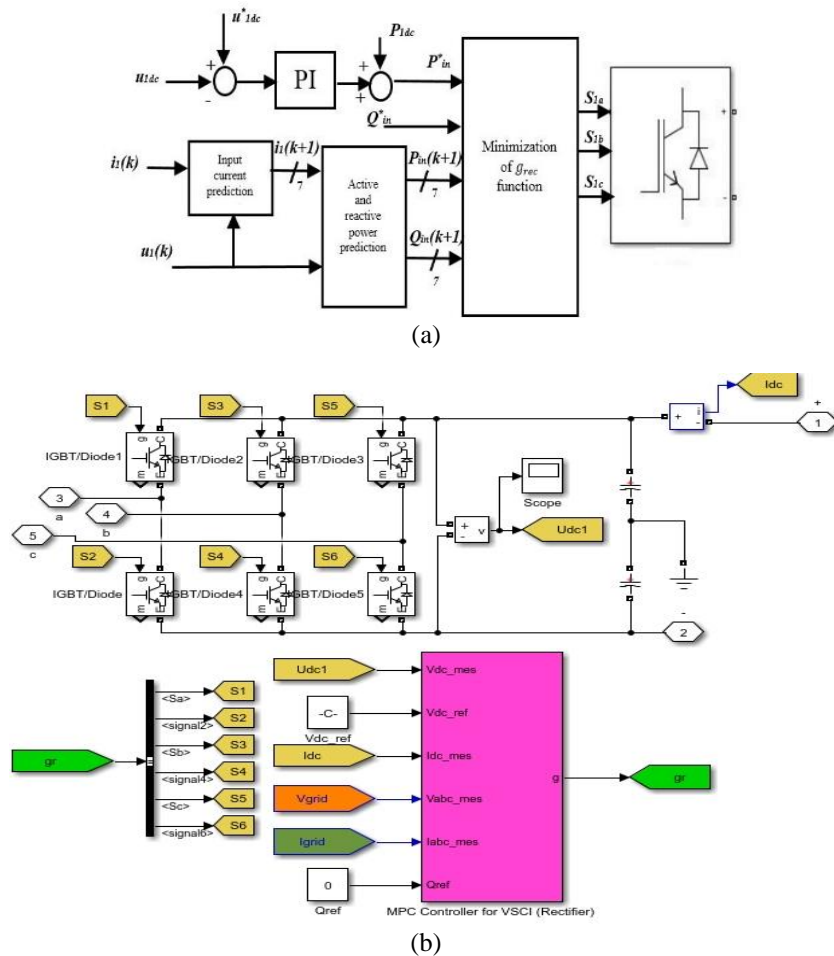


Figure 2. Predictive power control scheme for the rectifier: (a) block diagram and (b) Simulink model

### 3.2. Design scheme of rectifier side controller

The purpose of the current control is to reduce the static error. To satisfy this condition, (17) can be wrote as a cost function, which calculates the error between the references and the anticipated currents:

$$g_{inv} = |i_{1\alpha}^*(k+1) - i_{1\alpha}^p(k+1)| + |i_{1\beta}^*(k+1) - i_{1\beta}^p(k+1)| \quad (17)$$

where  $i_{1\alpha}^p(k+1)$  and  $i_{1\beta}^p(k+1)$  are the real and imaginary parts of the predicted load current vector  $i^p(k+1)$ . By assuming that  $i^*(k+1) \approx i^*(k)$ , this supposition can give a one-sample delay in the reference pursuit, which is not a problem if a high sampling period is considered. The block diagram and the designed Simulink model of the current control strategy for the inverter is given in Figures 3(a) and 3(b) respectively.

The basic steps of the predictive current control algorithm are as follows, see Figure 4: i) measure the controlled current ( $i_2(k)$ ) at the  $k$ th sampling period; ii) carry out the best switching state considered in the previous sampling frequency; iii) predict the output currents for all possible switching states for the upcoming  $(k+1)$ th sampling instant, based on the discrete time model; iv) determine the cost function for the predicted output currents based on the control objectives; and v) choose the switching state that decreases the cost function and stock it for using at the next sampling period.

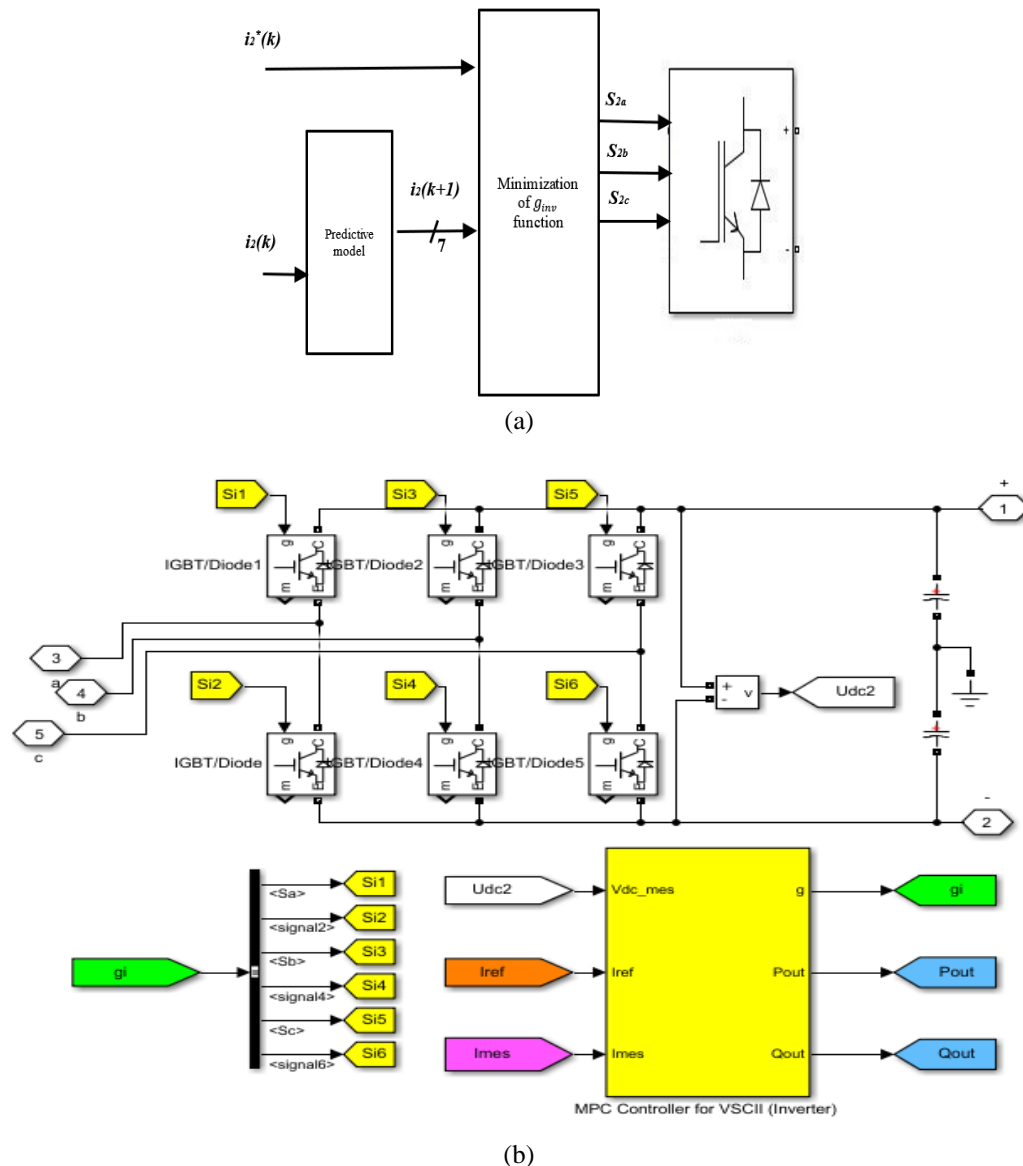


Figure 3. Predictive current control: (a) block diagram and (b) Simulink model

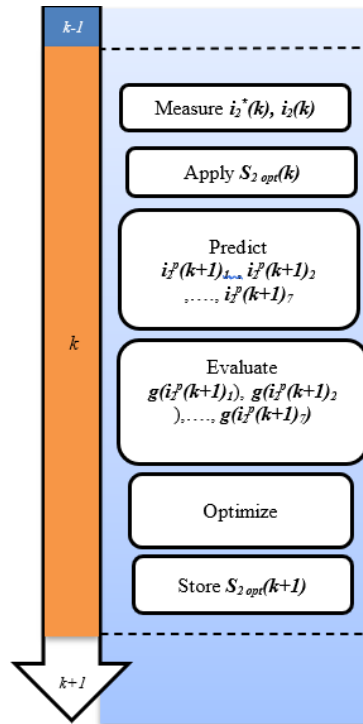


Figure 4. The predictive current control algorithm

#### 4. SIMULATION AND RESULTS

The simulation model of VSC based HVDC system is built in MATLAB/Simulink (with the help of MATLAB embedded system functions) to validate the model with predictive control method. The schematic layout used for simulation is given in Figure 5. The first converter (VSC-I) used to regulate powers, whereas the second converter (VSC-II) used to trace the AC current. Between two converters, a 100 km long transmission line model is also used; the simulation model is also built under the following parameters: The three-phase sending end line (base) voltage is set to 230 kV, rated (base) voltage of DC-side  $u_{1dc}=360$  kV, DC capacitor  $C_{dc}=6000$   $\mu$ F. The receiving end line (base) voltage is set to 230 kV; the base apparent power 800 MVA, the system frequency is set to 50 Hz and the sampling period is set to 25  $\mu$ sec.

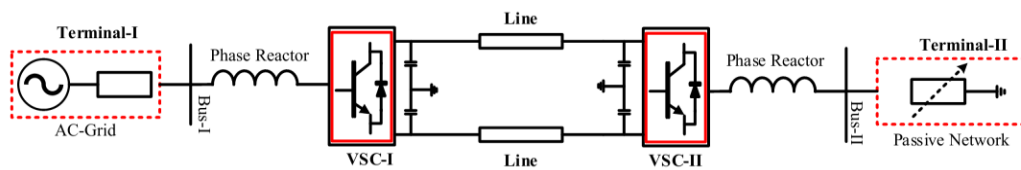


Figure 5. VSC-HVDC system used in our simulation

##### 4.1. Normal operation

The AC voltage of rectifier side is fixed to 1.0 pu (230 kV). The DC voltage is fixed to 1.0 pu (360 kV). The reactive power reference value is set to 0 pu (0 Mvar) and the active power reference value is set to 0.75 pu (600 MW). The following simulation waveforms are acquired at steady state. Allowing to Figures 6 and 7, the system in steady state has the following features:

- At rectifier side

The control approach of the rectifier part is to keep DC link voltage, active and reactive power on their setpoints values. It is identified from Figure 6, the first 0.1 s is the commencement process, and the DC link voltage slowly becomes stable at 1.0 pu that be given as shown in Figure 6(c). Also, Figure 6(d) illustrates that the active and reactive power are also stable at their given values. In addition, Figures 6(a) and 6(b) shows the input voltage and current respectively, in which they are sinusoidal waveforms and are also in phase.

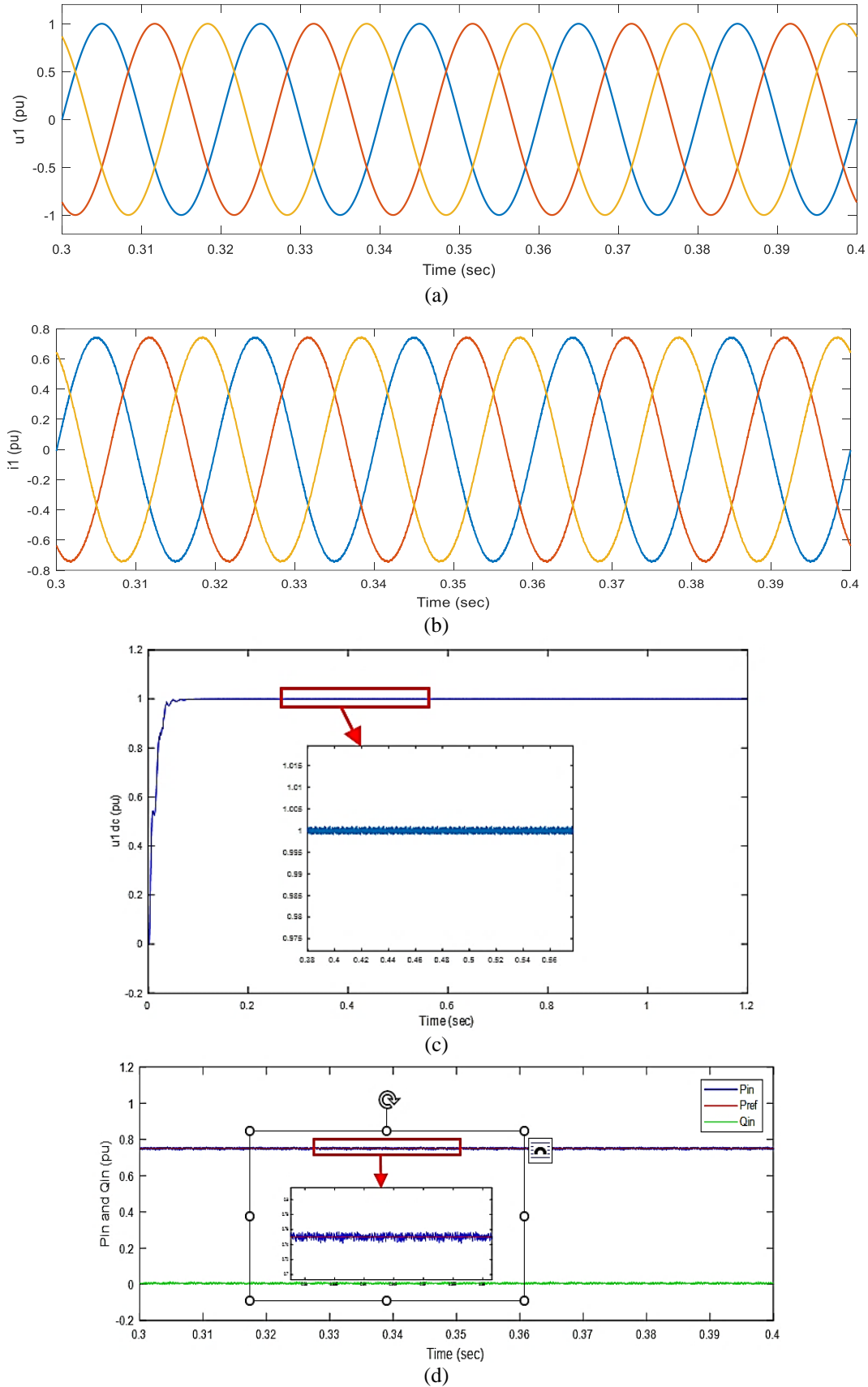


Figure 6. Rectifier side: (a) AC input voltage, (b) AC input current, (c) DC link voltage, and (d) input active and reactive power

– At the inverter side

The AC output voltage is sinusoidal signal and in phase with the output current  $i_2$ . The output current  $i_2$  tracks its reference value (which is around 0.74 pu, since we take in consideration the transmission line losses), as shown in Figure 7(a). Also, Figure 7(b) demonstrates that the active power is slightly less than the rated value; this is obvious because line parameters can influence the transmitted power over the DC link (since we are transmitting power to a passive network i.e. there is no compensation for the power losses). The output voltage  $u_2$  is almost a sinusoidal waveform and in phase to the output current as mentioned in Figure 7(c).

#### 4.2. Malfunction operation

In order to test the dynamicity and the fast response of the designed controllers, a disturbance/step response must be applied to a part of the whole system. The goal from those tests is to see the behavior of the fault's applied section (eg: the sending or receiving end) and its impact to the other end and vice versa. According to the previous arguments, we apply two step tests, the first is a step in the input AC voltage of -0.2 pu at  $t=1$  s; and the second one is a step of +0.25 pu in the reference output current at  $t=1$  s.

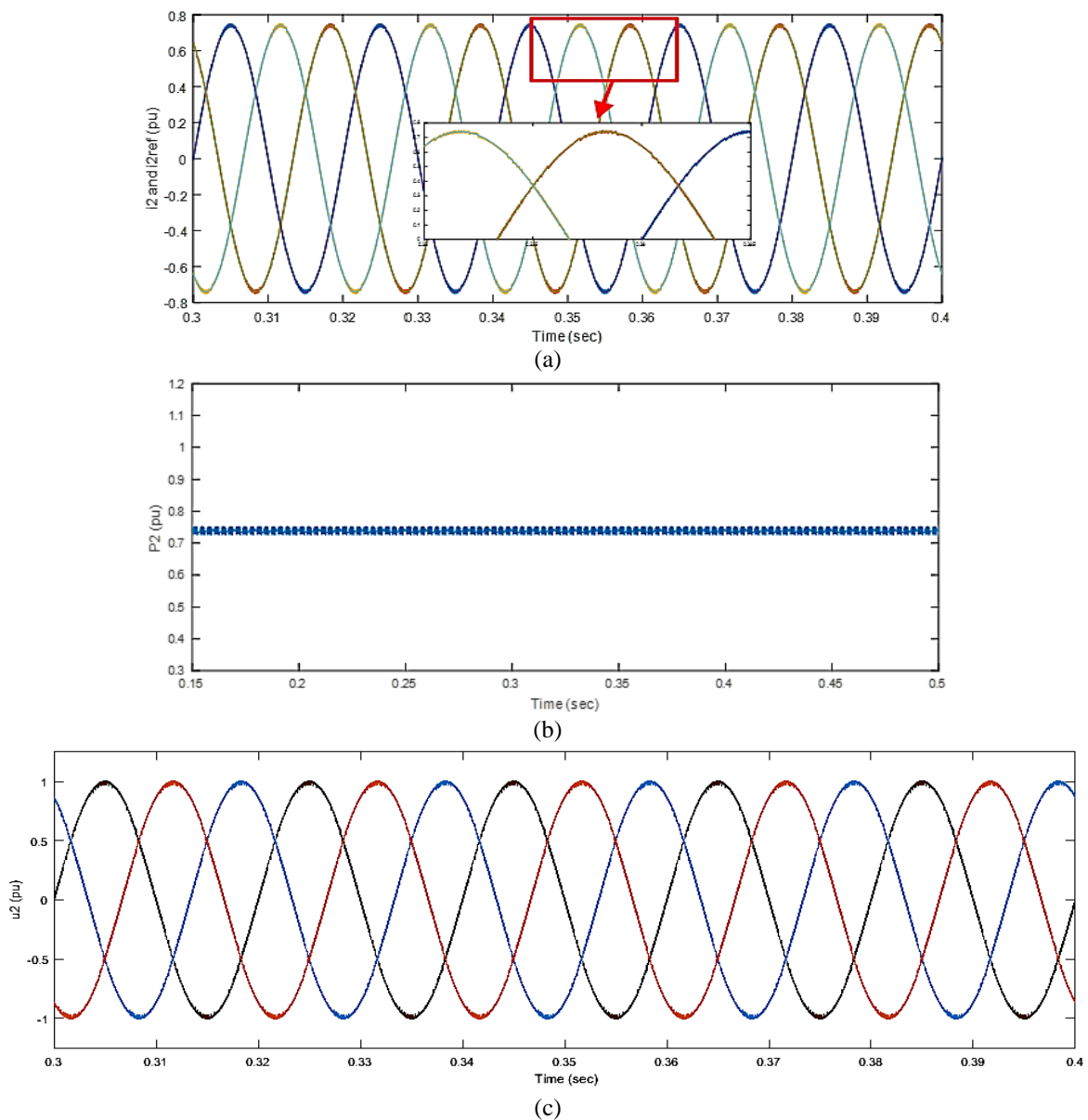


Figure 7. Inverter side: (a) AC output current, (b) output active power, and (c) AC output voltage

#### 4.2.1. Step in the input AC voltage ( $u_1$ )

After we apply a step of  $-0.2$  pu in the input voltage ( $u_1$ ) at  $t=1$  s (the fault is cleared after three cycles), the following results are obtained. Referring to Figure 8 we can deduce the following results:

– At rectifier side.

After the fault is applied at  $t=1$  s, the input voltage and current present a fast dynamic behavior to keep the controlled variables (the active and reactive power) at their reference trajectories seen from Figures 8(a) and 8(b) respectively, the active power showed two peaks of around  $-0.15$  and  $+0.15$  pu at the start and the end of the applied fault respectively, after the fault is cleared the active power restored to its stable state at  $0.75$  pu as shown in Figure 8(c), while the currents are kept sinusoidal and in phase with the supply voltages, even during the transient.

– At the inverter side.

All the waveforms at the inverter side is kept unchanged like the ones shown in Figure 7 (since the power transmitted over the DC link is kept almost constant during the fault).

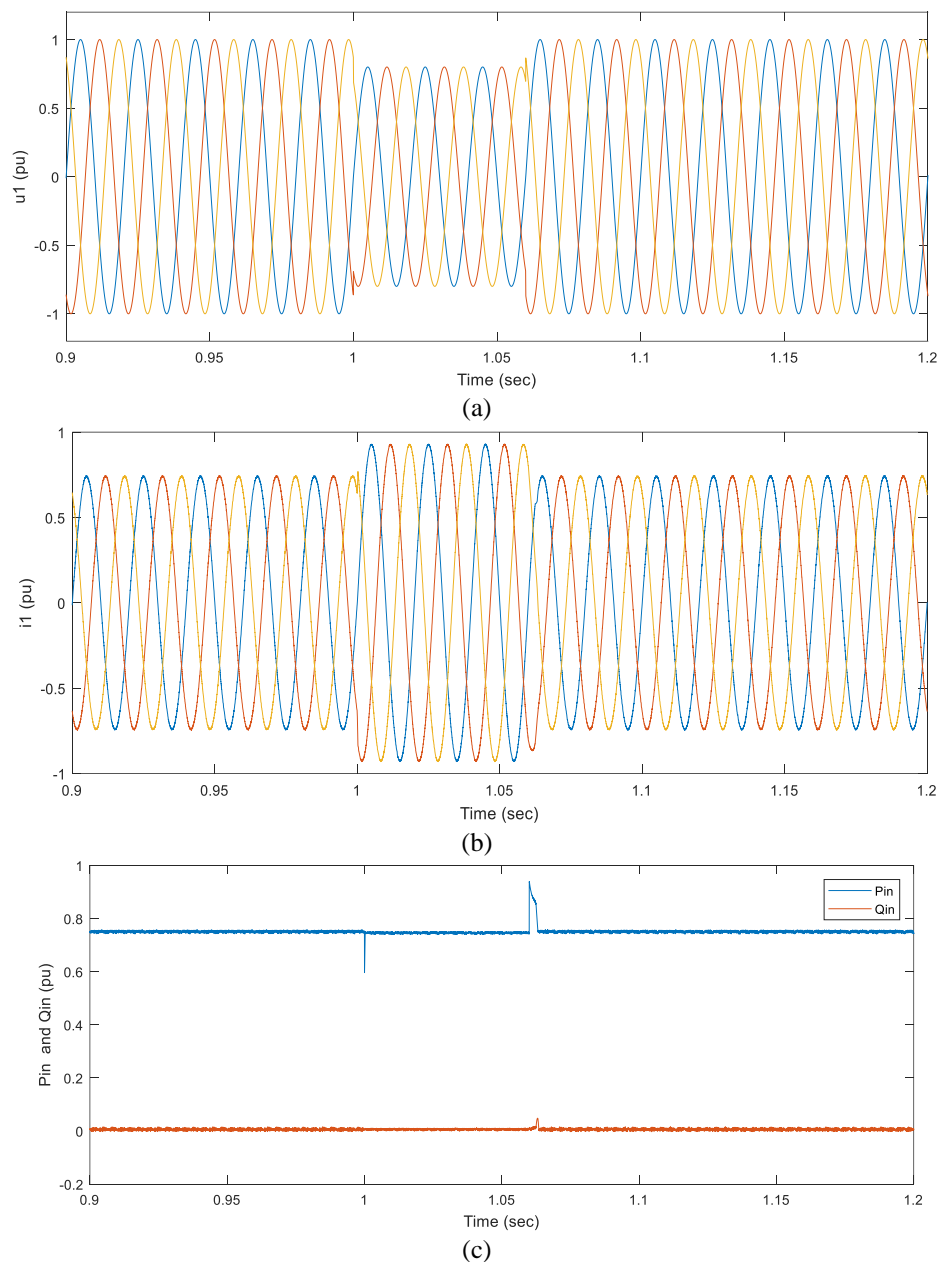


Figure 8. Comportment of the predictive power control in the input AC voltage of  $-0.2$  pu at  $t=1$  s (a) AC input voltage, (b) AC input current, and (c) input active and reactive power

#### 4.2.2. Step in the reference output current ( $i^*_2$ )

After we apply a step of +0.25 pu in the reference output current at  $t=1$  s, the following results are obtained. The comportment of the predictive control scheme of the load current reference is given in Figure 9. The inverter currents and active power react with fast dynamics to this variation (shown in Figures 9(a) and 9(b) respectively) that leads the rectifier to compensate the power needed, this is done by modifying the input active power setpoint. In addition, Figure 9(c) shows that the input currents has a fast dynamic performance. While Figure 9(d) demonstrates that the input active power has a good performance due to this variation while the transient does not disturb the reactive power.

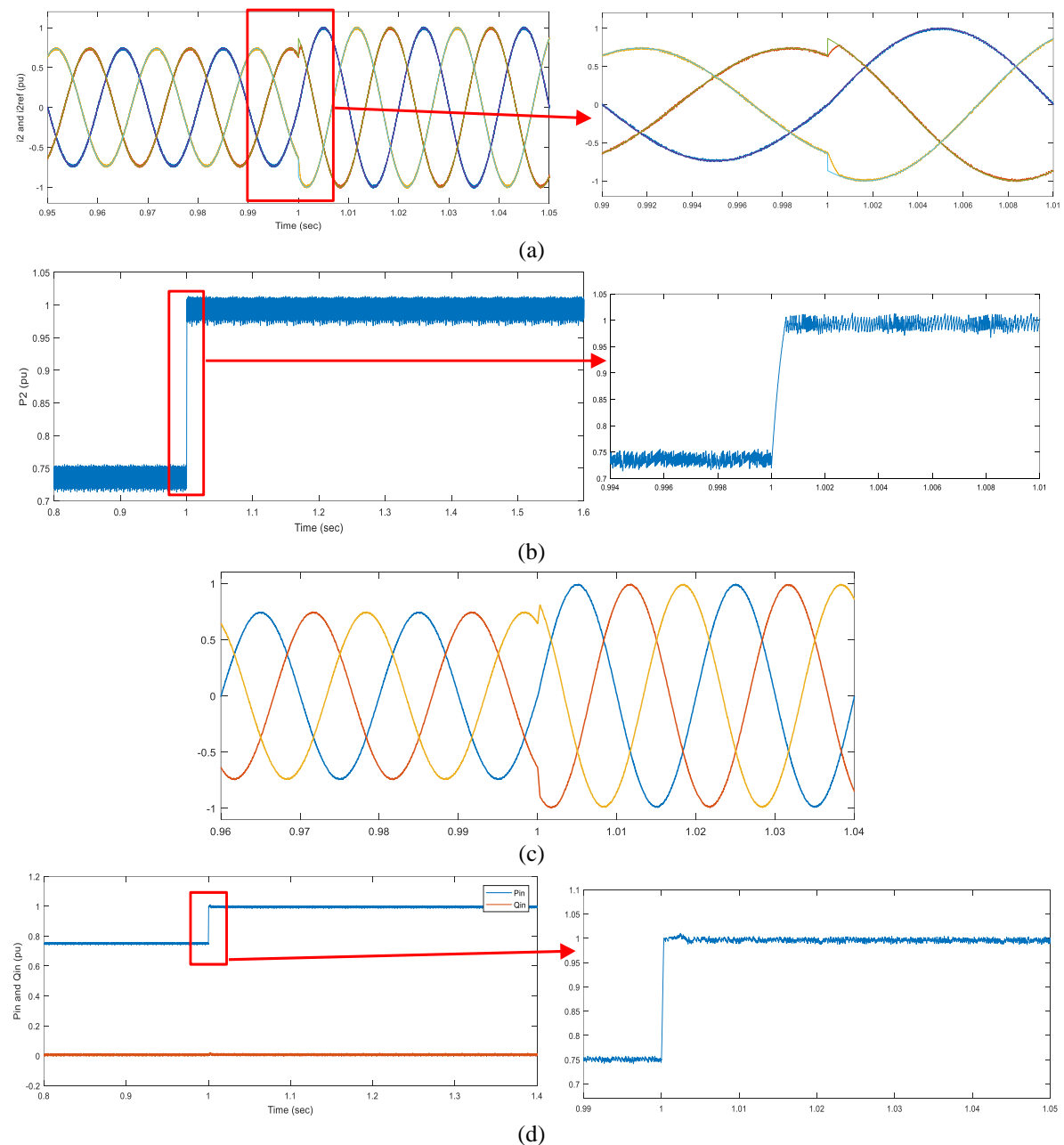


Figure 9. Comportment of the predictive power control (a) output AC current, (b) output active power, (c) AC input current, and (d) input active and reactive power

## 5. CONCLUSION

In this article, we have discussed the discrete mathematical model of the inverter and converter parts of the VSC-HVDC system; as well as their predictive control that is used to control and maintain the

controlled variable in their trajectories. Knowing that the predictive control uses a finite set of switching states: i) that can be produced by the power converters; ii) that are employed to anticipate the future comportment of the controlled variables (in our case the direct power flow at the rectifying station and a AC current at the inversion station) for each switching state; iii) the simplicity of the control structure since there is no complicate calculation or algorithms, also there is no inner loop current control which improves the system reliability; iv) fast dynamic response especially at faults, which gives the proposed control method a good advantage rather than the classical methods used before (eg: PI control); and v) good steady state performance.




## REFERENCES

- [1] R. Rogersten, "VSC-HVDC system modeling and validation," M.S. thesis, Department of Electrical Engineering, KTH University, Stockholm, Sweden, 2014.
- [2] D. P. Mishra, R. Senapati, and S. R. Salkuti, "Comparison of DC-DC converters for solar power conversion system," *Indonesian Journal of Electrical Engineering and Computer Science (IJECS)*, vol. 26, no. 2, pp. 648-655, May 2022, doi: 10.11591/ijeecs.v26.i2.pp648-655.
- [3] M. S. Ghayad, N. M. Badra, A. Y. Abdelaziz, and M. A. Attia, "Reactive power control to enhance the VSC-HVDC system performance under faulty and normal conditions," *International Journal of Applied Power Engineering (IJAPE)*, vol. 8, no. 2, pp. 145-158, 2019, doi: 10.11591/ijape.v8.i2.pp145-158.
- [4] Y. Zhu, "The VSC-HVDC electric power quality analysis and research," *CIREN 2012 Workshop: Integration of Renewables into the Distribution Grid*, 2012, pp. 1-4, doi: 10.1049/cp.2012.0766.
- [5] J. Setréus and L. Bertling, "Introduction to HVDC technology for reliable electrical power systems," *Proceedings of the 10th International Conference on Probabilistic Methods Applied to Power Systems*, 2008, pp. 1-8.
- [6] M. Morari and J. H. Lee, "Model predictive control: past, present and future," *Computers & Chemical Engineering*, vol. 23, no. 4-5, pp. 667-682, 1999, doi: 10.1016/S0098-1354(98)00301-9.
- [7] K. Mohamed, Z. S. Ahmed, Hadjeri Samir, F. M. Karim, and A. Rabie, "Performance analysis of a voltage source converter (VSC) based HVDC transmission system under faulted conditions," *Leonardo Journal of Sciences*, no. 15, pp. 33-46, 2009.
- [8] C. Guo and C. Zhao, "A new technology for HVDC start-up and operation using VSC-HVDC system," *2009 IEEE Power & Energy Society General Meeting*, 2009, pp. 1-5, doi: 10.1109/PES.2009.5275742.
- [9] R. S. R. Sankar, A. Venkatesh, and D. Kollipara, "Adaptive hysteresis band current control of grid connected PV inverter," *International Journal of Electrical and Computer Engineering (IJECE)*, vol. 11, no. 4, pp. 2856-2863, 2021, doi: 10.11591/ijece.v11i4.pp2856-2863.
- [10] P. K. Rath and K. C. Bhuyan, "Vector control of VSC HVDC system under single line to ground fault condition," *International Journal of Applied Power Engineering (IJAPE)*, vol. 7, no. 1, pp. 59-64, 2018, doi: 10.11591/ijape.v7.i1.pp59-64.
- [11] N. A. M. Yusoff, et al. "Analysis of direct power control AC-DC converter under unbalance voltage supply for steady-state and dynamic response," *International Journal of Electrical and Computer Engineering (IJECE)*, vol. 10, no. 4, pp. 3333-3342, 2020, doi: 10.11591/ijece.v10i4.pp3333-3342.
- [12] R. Heyderi, M. Alhasheem, T. Dragicevic, and F. Blaabjerg, "Model predictive control approach for distributed hierarchical control of VSC-based microgrids," *2018 20th European Conference on Power Electronics and Applications (EPE'18 ECCE Europe)*, 2018, pp. 1-8.
- [13] B. Saber, B. Abselkader, B. Mansour, and B. Said, "Sliding mode control of three levels back-to-back VSC-HVDC system using space vector modulation," *International Journal of Power Electronics and Drive System (IJPEDS)*, vol. 4, no. 2, pp. 265-273, 2014.
- [14] J. Rodriguez and P. Cortes, "Model predictive control," in *Predictive Control of Power Converters and Electrical Drives*, 1st ed., Chichester, U.K: John Wiley & Sons, Ltd, 2012.
- [15] A. Linder, R. Kanchan, R. Kennel, and P. Stolze, *Model-based predictive control of electric drives*, Göttingen, Germany: Cuvillier Verlag, 2012.
- [16] J. Rodriguez et al., "State of the art of finite control set model predictive control in power electronics," in *IEEE Transactions on Industrial Informatics*, vol. 9, no. 2, pp. 1003-1016, May 2013, doi: 10.1109/TII.2012.2221469.
- [17] S. Vazquez, J. Rodriguez, M. Rivera, L. G. Franquelo, and M. Norambuena, "Model predictive control for power converters and drives: advances and trends," in *IEEE Transactions on Industrial Electronics*, vol. 64, no. 2, pp. 935-947, Feb. 2017, doi: 10.1109/TIE.2016.2625238.
- [18] S. Kouro, P. Cortes, R. Vargas, U. Ammann, and J. Rodriguez, "Model predictive control—a simple and powerful method to control power converters," in *IEEE Transactions on Industrial Electronics*, vol. 56, no. 6, pp. 1826-1838, Jun. 2009, doi: 10.1109/TIE.2008.2008349.
- [19] I. S. Mohamed, "Implementation of model predictive control for three phase inverter with output LC filter using DSP," M.S. thesis, Faculty of Engineering, Cairo University, Cairo, Egypt, 2014.
- [20] M. P. Akter, S. Mekhilef, N. M. L. Tan, and H. Akagi, "Model predictive control of bidirectional AC-DC converter for energy storage system," *Journal of Electrical Engineering and Technology*, vol. 10, no. 1, pp. 165-175, 2015, doi: 10.5370/JEET.2015.10.1.165.
- [21] Y. A. Elthokaby, I. Abdelsalam, N. Abdel-Rahim, and I. M. Abdealqawee, "Model-predictive control based on Harris Hawks optimization for split-source inverter," *Bulletin of Electrical Engineering and Informatics*, vol. 11, no. 4, pp. 2348-2358, Aug. 2022, doi: 10.11591/eei.v11i4.3823.
- [22] I. M. Syed and K. Raahemifar, "Model predictive control of three phase inverter for PV systems," *International Scholarly and Scientific Research & Innovation*, vol. 9, no. 10, pp. 1188-1193, 2015.
- [23] Z. Massaq, A. Abounada, and M. Ramzi, "Fuzzy and predictive control of a photovoltaic pumping system based on three-level boost converter," *Bulletin of Electrical Engineering and Informatics*, vol. 10, no. 3, pp. 1183-1192, Jun. 2021, doi: 10.11591/eei.v10i3.2605.
- [24] H. Ikaouassen, A. Raddaoui, M. Rezallah, and H. Ibrahim, "Improved predictive current model control based on adaptive PR controller for standalone system based DG set," *International Journal of Electrical and Computer Engineering (IJECE)*, vol. 10, no. 2, pp. 1905-1914, 2020, doi: 10.11591/ijece.v10i2.pp1905-1914.




- [25] A. K. Ali and R. G. Omar, "Finite control set model predictive direct current control strategy with constraints applying to drive three-phase induction motor," *International Journal of Electrical and Computer Engineering (IJECE)*, vol. 11, no. 4, pp. 2916-2924, 2021, doi: 10.11591/ijece.v11i4.pp2916-2924.
- [26] M. Amine and M. Molinas, "Model predictive control of voltage source converter in a HVDC system," 2017, arxiv: 1704.04293.
- [27] X. Zhang, Y. Wang, C. Yu, L. Guo, and R. Cao, "Hysteresis model predictive control for high-power grid-connected inverters with output LCL filter," in *IEEE Transactions on Industrial Electronics*, vol. 63, no. 1, pp. 246-256, Jan. 2016, doi: 10.1109/TIE.2015.2477060.
- [28] P. Zhao *et al.* "Model predictive control of VSC-HVDC transmission system for power supply to passive networks," *E3S Web of Conferences*, vol. 136, no. 17, p. 02015, 2019, doi: 10.1051/e3sconf/201913602015.

## BIOGRAPHIES OF AUTHORS






**Nouir Ahmed**    was born in Eloued, on 1991, received his engineering degree in electrical engineering from the Institute of Electrical and Electronic Engineering at Boumerdes, M'hammed Bouggera University, Algeria, in 2013, and M.Sc. degree from the National School of Polytechnics-Oran, Algeria in 2016. Since 2017, he has been working toward the Ph.D. degree in predictive control systems under the supervision of Prof. Zebirate Soraya. His research interests include identification, modeling, digital control, and predictive control of new power converter topologies for power systems. He can be contacted at email: hmdlaid@gmail.com.



**Zebirate Soraya**    was born in Sidi Bel Abbes Algeria on 1965, she has received her M.S degree in Electronics from University of Sidi Bel Abbes, Algeria, in 2002, and her Ph.D. degree in 2006. She is a Professor in industrial maintenance and safety institute at university of Oran 2, Mohamed Ben Ahmed, Algeria and member of "SCAMRE" laboratory. Her research interests are in the intelligent control. She can be contacted at email: szebirate\_dz@yahoo.com.



**Chaker Abdelkader**    was born in Oran Algeria, on 1952, he has received his PhD degree in electrical engineering from Polytechnic Institute of Saint Petersburg Russia in 2002. He is a Professor in the Electrical Engineering Department at ENPO-MA, Oran, Algeria and director of "SCAMRE" laboratory. His research activities include control of large power systems, multi machine multi converter systems and unified power-flow controllers. His teaching themes are neural process control and real-time simulation of power systems. He is author and co-authors of many scientific publications. He can be contacted at email: chakera@yahoo.fr.